Journal of Energy Storage 154 (2026) 121301

Contents lists available at ScienceDirect

Journal of Energy Storage

journal homepage: www.elsevier.com/locate/est

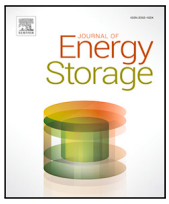

Research papers

The impact of battery scheduling strategies on profitability considering battery usage costs and dynamic electricity pricing in Nordic residential PV–battery system

Lauri Karttunen [a,*], Sami Jouttijärvi [a], Jerzy J. Jasielec [a,b], Johannes Niskanen [c], Hugo Huerta [d], Samuli Ranta [d], Kati Miettunen [a]

[a] Department of Mechanical and Materials Engineering, University of Turku, Vesilinnantie 5, 20014 Turku, Finland
[b] Department of Physical Chemistry and Modelling, AGH - University of Science and Technology, Al. Mickiewicza 30, Krakow 30-059, Poland
[c] Department of Physics and Astronomy, University of Turku, Vesilinnantie 5, 20014 Turku, Finland
[d] Department of Chemical Industry, Turku University of Applied Sciences, Joukahaisenkatu 7, 20520 Turku, Finland

ARTICLE INFO

Keywords:
Home energy management
Battery scheduling
PV–battery
MILP
Reinforcement learning

ABSTRACT

This study investigates (1) the economics of adding a battery to a residential photovoltaic (PV) system and (2) how different home energy management (HEM) strategies impact its profitability in a Finnish context. Our key novelty is the analysis on highly varying dynamic electricity prices from years 2020–2022 accompanied with the calculation of battery usage costs coming from battery degradation. Furthermore, by implementing multiple HEM strategies with variable complexity on real PV production and four real electricity consumption data, we provide a comprehensive study methodology. We tested five strategies, ranging from simple rule-based (SCM) to optimization (MPC) and reinforcement learning (RL) approaches. Our findings indicate that adding a typical 13.5 kWh/9000 EUR battery to a 4 kWp PV system is economically unfeasible for balancing the intermittent PV production under the current electricity prices in Finland. Two of the strategies considered battery usage costs in the decision making, leading to the battery staying unused, due to higher battery usage costs than electricity bill savings. The economic break-even battery capital expenditures (CAPEX) were 185 EUR/kWh at best under the high electricity prices of 2022. This is under a third of the given CAPEX of 667 EUR/kWh. Interestingly, the simple SCM resulted in practically equal electricity bill savings to complex MPC and RL in 2020–2021. However, during the elevated and highly varying prices in 2022, MPC achieved 5.7% lower electricity bills compared with SCM. Thus, complex HEM strategies were beneficial here only during volatile electricity prices.

1. Introduction

The prices of solar photovoltaics (PV) has decreased rapidly, leading to massive increases in installed PV capacity both globally and in high latitudes. Currently in Finland (2025), the national PV capacity is approximately 1.3 GWp [1], where majority are distributed small-scale production, such as residential PV systems. However, Finland currently has over 23 GWp utility-scale (> 1 MWp) PV plants either under construction or in authorization stage [2], implying massive increases to national more centralized PV generation. Since PV is variable renewable energy (VRE) technology with an intermittent production profile, energy storage is not only an attractive solution to increase the amount of self-consumed PV production, which increases the value of produced residential PV electricity [3], but also important for (1) reducing strain on grid due to the reverse power flow and high variation in the production, and (2) lowering the need of balancing power. Additionally, energy storage can provide energy security and uninterrupted power supply, and improve self-sufficiency.

Similarly than with PV, prices of batteries have decreased as well, and PV–battery systems have been reported to be economically profitable in some locations, such as in Switzerland [4,5] and Germany [6]. However, adding a battery to existing PV system has been shown in various locations to yet remain economically unprofitable, such as in Finland [7], Thailand [8], Madeira Island [9], Belgium [10], and Norway [11]. In addition to battery prices, local electricity prices affect the profitability of batteries. Especially, more volatile prices increase the economic profitability of battery, as has been shown by case studies from UK [12], and China [13]. Additionally, increasing purchase

* Corresponding author.
E-mail address: lauri.p.karttunen@utu.fi (L. Karttunen).

https://doi.org/10.1016/j.est.2026.121301
Received 22 August 2025; Received in revised form 10 February 2026; Accepted 20 February 2026
Available online 27 February 2026

price and decreasing feed-in price increase the economic profitability of home battery [10]. The profitability can be further improved by effective home energy management (HEM). The development of smart homes, due to the technologies such as advanced metering infrastructure (AMI), smart sensors, the Internet of Thing (IoT) home appliances, and smart grid technology, have made home energy management systems (HEMS) a crucial part of modern houses, allowing monitoring, controlling, and planning of the energy system devices [14]. The aim of HEMS is to provide efficient management of electricity production, storage, and consumption [15]. This work considers the management of production and storage, thus HEM is reduced to a battery scheduling optimization.

There are many approaches for battery scheduling, and HEM in general, which are extensively discussed in review works such as [16–18]. These approaches can be roughly categorized into rule-based, optimization, and machine learning (ML) methods. Rule-based HEM strategies are very common for battery scheduling because of their simplicity and low computational requirements. Especially, the self-consumption maximization (SCM) is a commonly used baseline strategy in real-world PV–battery applications. The operation principle of SCM is presented in Section 2.5. It is used for techno-economic analyses [7] and often used in benchmark studies for other strategies [19–23].

Optimization methods, on the other hand, are based on maximizing/minimizing the objective function over an optimization horizon, which is often 24 h [18,20,24,25]. The results of optimization are the scheduled actions of an energy system (*e.g.* battery) over the optimization horizon, which are based on forecasted variables, such as PV production and load. Various optimization methods for HEM have been used in literature, the most common ones being multi-integer linear programming (MILP), dynamic programming, and nature inspired meta-heuristic optimization methods [18]. Since optimization is based on forecasted variables, dealing with forecasting uncertainties is crucial. One approach to minimize the effect of forecasting uncertainties is to implement the optimization frequently, such as every hour, in which case only the first action of the optimized horizon is realized. This approach is called model predictive control (MPC) [18,25,26], and it can reduce the effects of forecast uncertainty [27], since only the nearest time step is realized. One of the drawbacks of optimization and MPC is the computational burden: HEM can be computationally very complex, and finding the global minimum might require tons of iterations.

Due to their adaptability and minimal computational requirements during operation, machine learning methods have gained popularity for HEM. Especially effective have been reinforcement learning (RL) methods, where an agent (which can represent a battery [28,29], for example) or multiple agents learn to operate effectively by using trial and error. The learning is guided by assigning rewards (or penalties) to actions, and these rewards are based on cost functions similar to those used in optimization. The advantages of RL over optimization are the computational speed after off-line training and its adaptability during online operation to maximize the expected future rewards [30,31], whereas optimization strategies are limited to the optimization horizon. In addition to RL methods, supervised learning ML models can be utilized by utilizing the optimized energy management patterns [19,24].

Objective functions for optimization and RL approaches of PV–battery systems are typically based on electricity bill minimization [32–35], but can also include other variables, such as user comfort [30,36,37] and battery degradation [20,22,38,39]. Although the electricity bill is an apparent indicator of economic savings, it is important to consider other effective costs, such as the battery degradation costs: battery usage affects its degradation and thus its lifetime and economic profitability. However, residential PV–battery studies with battery degradation costs under dynamic spot pricing over longer time periods are lacking. Ekhteraei Toosi et al. [38] showed that when total costs, including battery usage costs and electricity bill, were minimized instead of minimizing only electricity bill, monthly costs (electricity bill + battery usage costs) were reduced from 209 USD to under 46 USD. They studied a smart home with a 2.5 kWh battery, an electric vehicle (22 kWh battery capacity), and a 3 kWp PV system under spot pricing over a 1-month period. Zou et al. [20] implemented MPC with dynamic programming to a household with a 5 kWp PV system and a 12 kWh battery. By minimizing the total costs including the battery usage cost, they reduced the total costs from SCM results of 10.60 CNY to 9.36 CNY, over the studied 1-month period with ToU purchase tariff and fixed feed-in tariff. Abdulla et al. [39] showed that battery lifetime value can be improved on average by 160% over rule-based strategy, when battery degradation is included in the dynamic programming HEM strategy, by considering multiple existing households with variable sizes of PV systems and a simulated 5 kWh battery. This study also considered ToU purchase tariff and fixed feed-in tariff over 3-year period.

Correspondingly, HEM studies considering spot prices typically have simplified battery degradation cost model, or the degradation is neglected completely. Nygård et al. [11] concluded that a 10.2 kWh home battery was economically unprofitable under volatile 2022 electricity spot prices in Norway. Their battery CAPEX of 100,000 NOK (9800 NOK/kWh or around 980 EUR/kWh) lead to minimum economic payback time of 29 years from all studied consumer profiles. They concluded that a 30% investment support for batteries would lead to economic break-even. They used a fixed battery usage cost (NOK/kWh) for charging and discharging, which neglects the effects of cycle depth in the battery degradation. Huy et al. [24] showed that a neural network model trained from MILP optimized battery and EV charging patterns outperformed 24-hour optimization and RL methods. The work considered consumption and production data from UK during years 2012–2014, but battery degradation was neglected. Bozchalui et al. [40] compared various optimization objectives for HEM with fixed-rate plan (FRP), ToU, and dynamic pricing in Ontario (Canada) using MILP, but omitted battery degradation. With dynamic pricing, they showed that daily energy costs can be significantly reduced compared to ToU or FRP pricing. J. Salpakari and P. Lund studied rule-based SCM and optimization-based cost minimization control strategies for a heat pump, thermal and electrical storage, and load shifting in a low energy residential building with PV in Southern Finland using spot prices in 2013 [41]. They obtained maximum of 25% electricity bill savings compared with SCM, but battery costs and degradation were neglected. Shivam et al. [42] applied multi-objective optimization for step-ahead (1-hour horizon) battery scheduling of residential system with 14.5 kWp PV system and 9.6 kWh battery in Taiwan to flat and dynamic pricing, both scenarios with a fixed feed-in tariff. They compared various PV production and consumption forecast models from Naïve forecasting to ML-based forecast models. Under dynamic pricing, they showed that the optimized operation based on ML-forecasts increased the profits by up to 260% compared with not controlled energy management (supposedly SCM, although authors do not describe the model), while optimization with Naïve predictor increased the profits by 222%. However, battery degradation was not considered.

The objectives of this work are to discover if (1) adding a battery is economically feasible within these conditions and (2) how much different HEM strategies for battery scheduling affect the total costs. The first objective contributes to the understanding of home battery profitability in high latitudes, while the second objective is important for knowing how much profits can be increased by adding model complexity to HEM.

This work distinguishes itself from the existing literature [3–46] through a combination of methodological breadth, realistic data use, and novel transparency measures. While dynamic or time-varying pricing has been addressed in multiple studies [3,4,7,11,12,22,28,30,33,40,41,43–45], holistic studies under dynamic spot pricing that also account for battery usage cost due to degradation are lacking. This

Fig. 1. PV system of TUAS, used as the production data source.
Source: Photo by Anttalainen/UTU.

gap is particularly evident in the Nordic context, where no comparative studies exist that evaluate different HEM strategies with battery usage costs. The present analysis is timely because increasing installed VRE capacity affects both intra-day and annual mean electricity prices. Furthermore, the 2021–2023 energy crisis — driven by reduced energy production capacity following COVID-19 lockdowns and the disruption of gas and oil supply from Russia after its invasion of Ukraine — demonstrated how global events can drastically increase the volatility and magnitude of spot prices. By using three years of dynamic spot price data (2020–2022), this work covers both stable and extreme market conditions in a way that few studies have attempted.

Battery degradation modeling is another area where this work advances the state of the art. Although some prior research [11,20,22,28,32,37–39,43,45,46] incorporates degradation costs into optimization, many studies simplify or ignore these effects — particularly under spot pricing. This work integrates battery aging costs directly into the optimization function, enabling operational strategies that reflect real-world lifecycle impacts. Additionally, it systematically compares five distinct HEM strategies — including rule-based, model predictive control, and reinforcement learning approaches — two of which consider degradation in decision-making. While some earlier works [19,28,30,31,36,37,42,43] benchmark advanced methods against simpler ones, comprehensive comparisons of this breadth remain rare.

Geographically, this work focuses on Turku, Finland, a representative high-latitude location with Nordic climatic conditions and dynamic spot prices — both of which strongly influence HEM outcomes and battery profitability. High-latitude summers allow for diverse PV installation angles to be viable due to a better temporal match between production and consumption profiles [3], while winter conditions significantly limit PV output unless batteries are charged from the grid. Additionally, the PV production profile of differently oriented systems can influence battery degradation and thus the battery profitability [43]. Increased Nordic wind capacity, along with growing PV installations, has also made negative spot prices more common. In this setting, only a handful of studies [7,46] utilize measured household load and PV profiles in Nordics, and this work is among the very few to use multiple real households over several years.

Economically, the study aligns with a limited group [6,8–10,12,43] that calculate break-even CAPEX, but uniquely combines this with multi-year, dynamic-price, degradation-aware simulations. Notably, it is the only study to release its full simulation code as open-source [47], addressing a major reproducibility gap identified in the literature [3–41]. This transparency, combined with its emphasis on counter-intuitive findings — such as cases where battery use can increase total costs when degradation is neglected — makes the contribution both practically relevant and methodologically robust.

In summary, this work presents a comprehensive case study on adding a battery to residential households with existing PV in a Finnish high-latitude context, characterized by Nordic climate and dynamic spot electricity prices. The analysis uniquely combines:

- **Five HEM strategies** — rule-based, model predictive control (MPC), and reinforcement learning (RL) approaches, with two strategies explicitly considering battery degradation in decision-making.
- **Real-world data** — PV production and four measured household consumption profiles, capturing inter-household variability often omitted in prior Nordic studies.
- **Multi-year dynamic pricing** — three years of day-ahead spot prices (2020–2022), spanning pre-crisis stability, COVID-related impacts, and the 2022 energy crisis driven by reduced production capacity and fuel supply disruptions.
- **Degradation-aware optimization** — battery usage costs directly included in the optimization objective, producing lifecycle-realistic operation schedules.
- **Economic feasibility assessment** — break-even CAPEX calculated under varying price conditions, linking technical performance to financial viability.
- **Transparent methodology** — complete simulation code released as open-source [47], enabling reproducibility and transferability to other contexts.

This integrated approach fills significant literature gaps by jointly analyzing multi-year dynamic pricing, battery degradation costs, and a diverse set of HEM strategies in a Nordic setting, offering both technical and economic insights directly relevant to future PV–battery deployments.

2. Methodology

2.1. Data

Production

Our PV production data was obtained from a PV system installed by the Turku University of Applied Sciences (TUAS) on the roof in Turku, Finland, at coordinates 60.447 ° N, 22.298 ° E. The system consists of 18 Kingdom Solar KD-250 polycrystalline modules [48], installed toward south in a 15 degrees tilt. The system is installed on an industrial building at an elevation of 28 m above sea level, including the building itself standing 9 m tall. There is moderate shading, primarily caused by two trees located 15 m from the south-west and the IV room situated 2.5 m to the east, causing around 3.5% shading losses annually. Data was collected every 5 min, allowing for detailed monitoring and analysis of the solar energy production. This data is openly available at Ref. [49]. The system is presented in Fig. 1.

The rated power P_0 of the PV system was 4.5 kWp. We scaled the production from the DC side before inverter so that P_0 is 4 kWp, in order to have a comparable system size to our other works covering residential PV installations in Finland [3,50]. This sizing is reasonable, since the monthly production during the high production months of

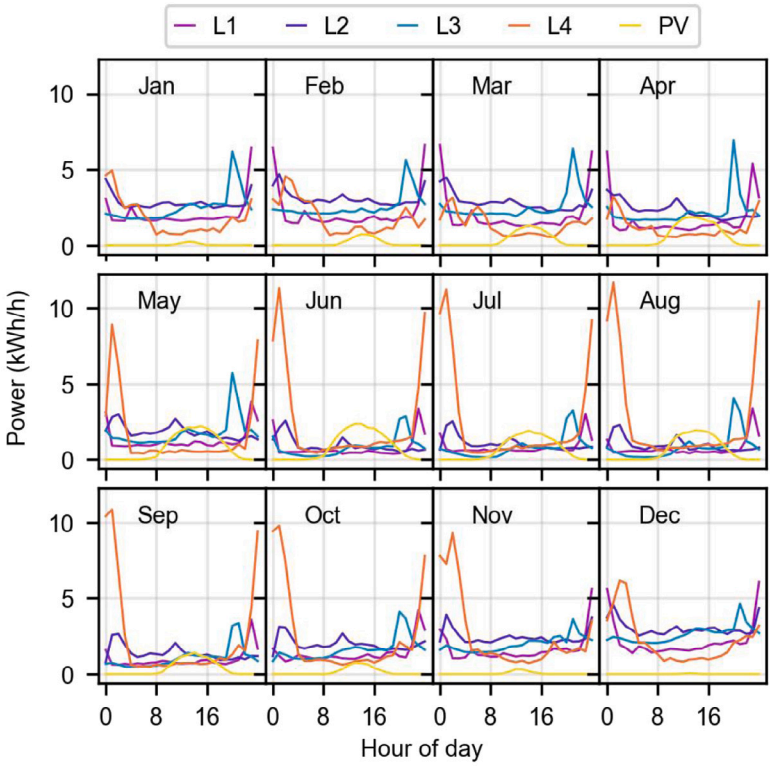

Fig. 2. Monthly average electricity consumption along load profiles 1–4 and the PV power, presented for each hour of a day using data from 2020.

June and July match the monthly consumption for L1–L3. Overproduction during these months would lead to selling of the production, which is economically not as beneficial as self-consumption [3,50]. To obtain AC power, we reduced the DC power readings by 3%, assuming a constant 97% inverter efficiency. The studied system did not experience any inverter clipping. To filter out possible erroneous power data, we excluded datapoints that had AC power outside $[0, 1.02 \cdot P_0]$, where 1.02 upper filter is based on IEC standards [51,52]. After this, we aggregated the 5-minute data to hourly data by taking an hourly mean for hours with at least six not-missing datapoints. If an hour contained more than six missing datapoints, the power on that hour was set to 0. This procedure was applied because high missing data rates within an hour indicates some sort of data logging issue, which could compromise the power readings. This affected only a total of 142 h, which had a mean power of 0 before the procedure, and therefore it did not affect the power profile.

Consumption

We employed hourly electricity consumption data collected from four real individual households over 2020–2022 across Turku area, referred here as L1–L4. The mean daily consumption and production profiles for each month are presented in Fig. 2, obtained using data from 2020. Additionally, Fig. 3A shows the annual consumption and production yields and Fig. 3B the monthly consumption and production. From Fig. 3B, the PV sizing criterion of matching the summer month production and load, is visible.

Without further information on the housing and heating type for loads L1–L3, the high annual consumptions over 10 MWh indicate that all consumers are detached houses. Based on the monthly consumptions in Fig. 3B, the increased consumption during winter months suggest that loads L1–L3 have electric heating. These three profiles have a load peak in the evening or during night (Fig. 2), which can be caused by lumped usage of home appliances, or heating the house and/or domestic hot water. L4 is a detached house with reserving heating that can utilize either electricity or wood. Additionally, L4 has an electric car, which causes peak loads during night-time (Fig. 2). In this work, we considered only battery usage without load management, and therefore accurate knowledge on the usage patterns of home appliances and heating solution can be neglected.

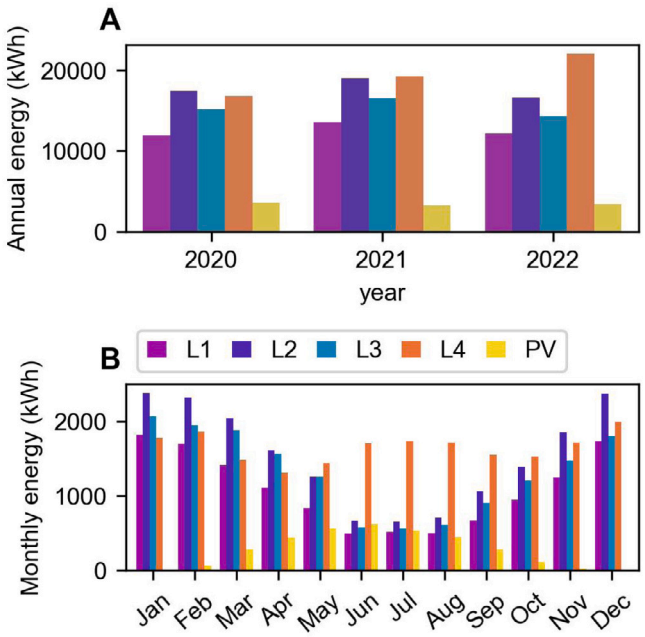

Fig. 3. Electricity consumption for the load profiles 1–4 and the PV production yield A: in annual scale, B: in monthly scale (obtained as monthly means over all years 2020–2022).

Electricity contract

For all consumers, we implemented spot price based electricity contracts, where the purchase and sell prices p_{purch} and p_{sell} are defined

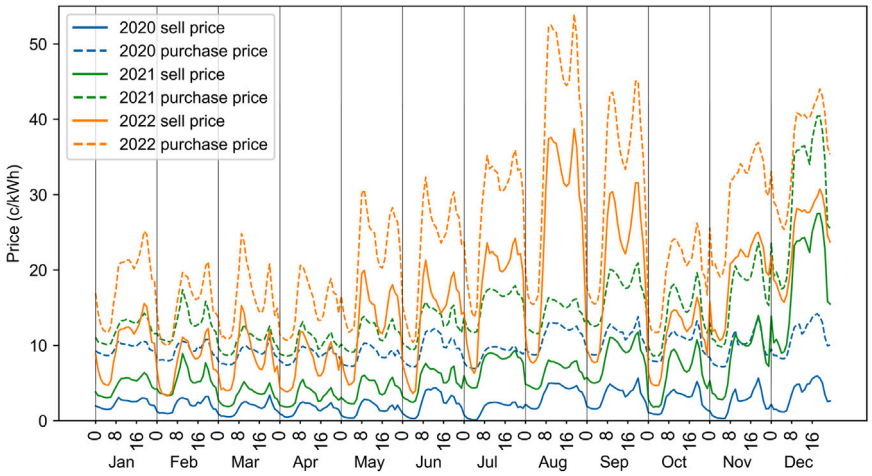

Fig. 4. Average purchase (dashed lines) and sell (solid lines) prices for each hour within each month, on years 2020 (blue), 2021 (green), and 2022 (orange). The shown values are the average prices for the particular hour of the day during the ongoing month. E.g., the value at location '8' for the month May is the average electricity price on May 1st–May 31st at 8–9 am. (For interpretation of the references to color in this figure legend, the reader is referred to the web version of this article.)

Table 1
Electricity price components for the different years in the unit of c/kWh.

Price component	2020	2021	2022
$p_{\text{trans+tax}}$	5.90	5.44	5.01
p_{margin}	0.4	0.4	0.4
p_{spot} (avg.)	2.89	7.23	15.40
p_{purch} (avg.)	9.19	13.07	20.81
p_{sell} (avg.)	2.49	6.83	15.00

as follows:

$$p_{\text{purch}} = p_{\text{spot}} \cdot (1 + \text{VAT}) + p_{\text{trans+tax}} + p_{\text{margin}} \quad (1)$$

$$p_{\text{sell}} = p_{\text{spot}} - p_{\text{margin}}, \quad (2)$$

where p_{spot} is the spot price, VAT is the value added tax of 24%, $p_{\text{trans+tax}}$ is the fixed transmission cost, including the supply security fee and electricity tax, and p_{margin} is a small fixed cost. The spot price determined by the Nordpool electricity markets varies hourly and can have negative values. The transmission cost is assigned by the local grid company, and the margin is determined by the electricity company — these costs are fixed and always positive. The total electricity price varies when the electricity is used. We used a p_{margin} of 0.4 c/kWh, which is a typical value for this component. Fixed cost $p_{\text{trans+tax}}$ depends on the location, year, and customer load type. Values used in this study for each load are presented in Table 1. They correspond to the average customer type values by the Finnish Energy Authority [53]. For all loads, we used values presented for detached house with partly reserving electric heating, main fuse size of 3x25 A, annual electricity consumption of 20 MWh, and Turku Energia Sähköverkot Oy grid company. Year 2020 was missing from the data, thus we used the same values as in 2019 (5.90 c/kWh).

In Fig. 4 , the average hourly electricity sell and purchase prices are shown for each month and years. At the end of year 2021, there is a rapid increase in the spot prices due to the energy crisis, which resulted elevated electricity prices also during 2022. During these high electricity prices, it can be seen that on average, the electricity selling prices during days can be even significantly higher than the purchase prices during nights. This difference in the prices mean that it can be more profitable to sell excess production during days than store it and use during night. The annual mean spot, purchase, and sell prices are presented in Table 1.

Table 2
The parameters of simulated Powerwall battery [54]: P^{MAX}: maximum charge/discharge power, η_{RT}: round-trip efficiency, $E^{\text{MAX}}_{\text{B,init}}$: initial nameplate battery capacity, C_{CAPEX}: capital expenditures, including installation. CAPEX was obtained from source [55].

Variable	P^{MAX}	η_{RT}	$E^{\text{MAX}}_{\text{B,init}}$	C_{CAPEX}
	(kW)	(-)	(kWh)	(EUR)
Value	5	0.9	13.5	9000

2.2. Energy system simulation

For the energy management simulation, we used the scaled real 4 kWp PV production and electricity consumption data (described above), as well as the day-ahead spot price data. The simulated battery was chosen to represent Tesla's Powerwall 2 [54], and the used parameters are presented in Table 2, where the battery capital expenditures (CAPEX) were estimated from Finnish mainstream media [55]. The size of 13.5 kWh is sufficient to move the excess production during daytime to evening and nighttime. The battery should not be too large, since oversized battery would lead to only partial battery cycling with higher CAPEX. As can be seen from Fig. 2, the consumption peaks during evening/night in all loads, thus the battery should be large enough to be able to store enough energy to cover those peaks and nighttime consumption. Only L4 has power peaks exceeding the maximum battery power of 5 kW during summer months, and those cannot be fully covered with the battery. For both PV and battery, separate inverters with 97% efficiencies were assumed. The system diagram is presented in Fig. 5. The battery was allowed to charge using PV production only.

The battery charge E_{B} for the next hour was obtained using the efficiency, and charge/discharge energies:

$$E_{\text{B}}(t+1) = E_{\text{B}}(t) + \eta E_{\text{CH}}(t) - \frac{1}{\eta} E_{\text{DCH}}(t), \quad (3)$$

where E_{CH} and E_{DCH} are the charged and discharged electric energies, and $\eta = \sqrt{\eta_{\text{RT}}}\eta_{\text{inv}}$ is the total efficiency, including the battery round-trip efficiency and inverter efficiency. We assumed the charge and discharge efficiencies to be equal by taking the square root of the round-trip efficiency, because they are close to each other [56–58], and since it is a common assumption in battery simulations, such as in [4,5,7,19]. To get the total efficiency of charging and discharging, both inverter and battery efficiencies have to be considered. To prevent discharging from

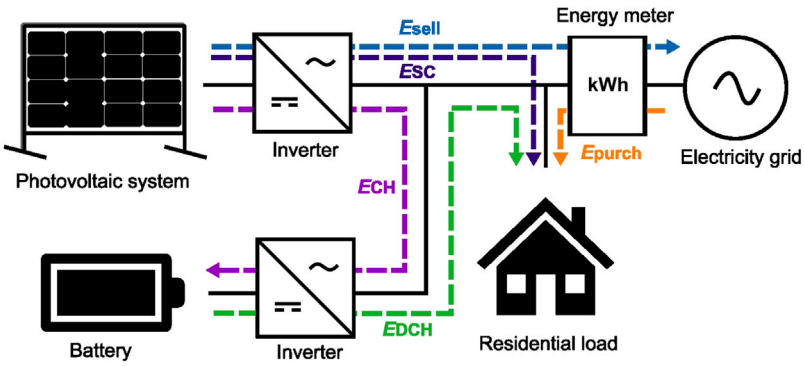

Fig. 5. Schematic diagram of the simulated system with possible electric energy flows. E_{CH}: charged electricity, E_{DCH}: discharged electricity, E_{SC}: self-consumed production, E_{sell}: sold production, E_{purch}: purchased electricity.

empty battery and charging battery over its capacity, the following constraints were applied for given hour:

$$0 \leq E_{CH} \leq \text{MIN}\left(E_{PV}, P^{MAX}\Delta t, (E_B^{MAX} - E_B)/\eta\right) \tag{4}$$

$$0 \leq E_{DCH} \leq \text{MIN}\left(\eta E_B^{MAX}, P^{MAX}\Delta t\right), \tag{5}$$

where E_{PV} is the PV production, P^{MAX} is the maximum battery charge/discharge power, Δt is the simulation resolution (1 h), and E_B^{MAX} is the battery capacity. Our consumption data is one hour resolution, since net metering has been and still is often done on hourly basis. Additionally, hourly based analysis is a common resolution in the literature, such as in [8,11–13,18,22,24,25,28,30,32,34,36,37,41–43,45,46].

2.3. Battery degradation modeling

A battery degrades during its lifetime, which leads to a decrease in its capacity and an increase of its resistance. In lithium-ion batteries, the main aging mechanisms are cracking and decomposition of cathode material and the formation of a thin cover layer on the anode side composed of the salt, electrolyte and cathode decomposition products [59–65]. This is often accompanied by gas build-up that causes cell swelling, worsens contact between electrode particles, and increases pressure, leading not only to cell failure but also to the risk of rupture [66]. Battery degradation progresses faster at high current rates, deep discharge conditions, as well as at low and high operating temperatures [67].

The degradation of the battery can be differentiated into the cyclic aging that describes loss of life due to battery operation (charging and discharging at different cycle depths (ΔSOC)) and float aging that occurs due to the progress of time (and depends primarily on temperature and state-of-charge (SOC)).

The capacity fade of the battery and the estimated End of Life (EoL) are important factors that need to be considered, when estimating the performance and costs of a battery used in HEM. The EoL of a battery is usually defined as the moment, when the capacity has decreased 20% from the initial capacity or when the internal resistance gets doubled [19,68]. For simplicity, we considered only the capacity fade and neglected the effects on the internal resistance in this work. As an effect of this simplification, the efficiency of the battery is assumed to be constant during the battery life-time and equal to the round-trip efficiency provided by the producer [54]. This approach is shared with other battery simulations described in the literature, such as [4–6,20].

Using the aging factor $c(t)$, the capacity at timestep t can be obtained as:

$$E_B^{MAX}(t+1) = E_B^{MAX}(t) \cdot (1 - x \cdot c(t)), \tag{6}$$

where x is the EoL capacity loss, and here we used the typical 20% EoL decrease, in which case $x = 0.2$. The change in state-of-health (ΔSOH) can be then calculated as:

$$\Delta\text{SOH}(t) = \frac{E_B^{MAX}(t) - E_B^{MAX}(t+1)}{E_{B,init}^{MAX} \cdot x} = \frac{E_B^{MAX}(t) \cdot c(t)}{E_{B,init}^{MAX}}, \tag{7}$$

where $E_{B,init}^{MAX} = E_B^{MAX}(0)$ is the initial nameplate value of the battery capacity. The EoL is encoded in the aging factor c, as will be presented below, and thus x cancels out in Eq. (7).

In some works, such as [19,21,44], the aging factor $c(t)$ is obtained as the sum of the cyclic and float aging factors, $c_{cyc}(t)$ and $c_{float}(t)$, respectively. However, in this work, only the predominant aging mechanism accounts for the total aging, according to the model we use in this work, given by Magnor et al. [68] and other works [45,46], such that

$$c(t) = \max\left(c_{cyc}(t), c_{float}(t)\right). \tag{8}$$

Cyclic aging

The relation between the maximum number of half-cycles N_{max} with a certain ΔSOC is usually given in the form of a Wöhler curve [68], which is often provided by the cell producer, or approximated with various semi-empirical models [68–72]. In this work, we used the Wöhler curve given by Magnor et al. [68], describing the maximum number of cycles as:

$$N_{max} = a \cdot \Delta\text{SOC}^b \tag{9}$$

where a and b are the fitting parameters calculated from the Wöhler curve, with the values of $a = 1.2698 \cdot 10^6$ and $b = -1.3133$, and ΔSOC is given as a percentage between 0–100.

For one cycle with a cycle depth ΔSOC, the cyclic aging factor $c_{cyc}^{full}(t)$ can be expressed as [68]:

$$c_{cyc}^{full}(t) = \frac{1}{N_{max}(\Delta\text{SOC}(t))}. \tag{10}$$

Assuming the same degradation from charging and discharging, c_{cyc} for a half-cycle is

$$c_{cyc}(t) = \frac{1}{N_{max}(\Delta\text{SOC}(t))}\frac{1}{2}, \tag{11}$$

where half-cycle means one continuous charge or discharge period, which may include idle periods, and timestep t is the end point of such half-cycle. Otherwise, if t is not an end-point of a half-cycle, $c_{cyc}(t) = 0$.

Float aging

The impact of the temperature follows the Arhenius' law, where the increase of temperature by ΔT (typically 10 to 15 kelvins) halves the lifetime. Hence, temperature-dependent aging factor c_T can be expressed as [68]:

$$c_T(t) = \frac{1}{t_{ref}} \int_{t_0}^{t_1} 2^{\frac{T(t)-T_{ref}}{\Delta T}} dt \tag{12}$$

where $T(t)$ is the battery temperature, t_{ref} is a reference calendar lifetime measured at the reference temperature T_{ref}, and t_0 and t_1 are the start and end time of the assessment period. In this work, we made a simplification by assuming that the battery operates at the reference temperature constantly. By assessing c_T every hour, *i.e.*, $t_1 - t_0 = 1$ hour, and assuming a calender lifetime of 15 years, similarly than in [68] at the reference temperature, each year containing 8760 h, c_T is reduced to the following time-invariant value:

$$c_T = \frac{1}{15 \cdot 8760}. \tag{13}$$

The aging dependence on the SOC is described using the SOC-dependent aging factor c_{SOC}, approximated using an exponential function [68]:

$$c_{\text{SOC}}(t) = \frac{1}{\alpha + \beta \cdot \exp(\gamma \cdot (100 - \text{SOC}(t)))} \tag{14}$$

where $\alpha = 2$, $\beta = -1.2$, and $\gamma = -0.0275$ are fitting parameters, and SOC is given as a percentage between 0–100. The float aging factor c_{float} is a product of c_T and c_{SOC}:

$$c_{\text{float}}(t) = \frac{1}{\alpha + \beta \cdot \exp(\gamma \cdot (100 - \text{SOC}(t)))} \cdot \frac{1}{15 \cdot 8760}. \tag{15}$$

2.4. Battery usage cost

Battery usage cost due to degradation C_{BAT} can be estimated using the given ΔSOH and battery investment costs C_{CAPEX} [45,73]:

$$C_{\text{BAT}}(t) = C_{\text{CAPEX}} \cdot \Delta\text{SOH}(t), \tag{16}$$

where C_{CAPEX} is the capital expenditures of the battery. We used C_{CAPEX} of 9000 EUR, which represents the CAPEX of Tesla's Powerwall in Finland [55]. This leads to specific battery cost of 667 EUR/kWh. C_{BAT} represents the total capital costs of the battery during its lifetime calculated for each hour (timestep). This allows us to include the battery degradation in the loss functions of HEM strategies.

Because these battery usage costs are linearly dependent on the battery CAPEX (Eq. (16)), it is possible to evaluate the break-even CAPEX, which leads to battery usage costs equal to the electricity bill savings. This break-even can be assessed by dividing the electricity bill savings (compared with NO-BATTERY scenario) by ΔSOH:

$$C_{\text{CAPEX,break-even,strategy}} = (C_{\text{el,bill,NO-BAT}} - C_{\text{el,bill,strategy}})/\Delta\text{SOH}, \tag{17}$$

where $C_{\text{el,bill,SCM}}$ is the annual electricity bill with NO-BATTERY strategy and $C_{\text{el,bill,strategy}}$ is the electricity bill with a given HEM strategy. The relative CAPEX in the unit EUR/kWh can be obtained by dividing the result of Eq. (17) with the battery capacity $E^{\text{MAX}}_{\text{B,init}}$.

2.5. Energy management methods

We applied five various energy management methods for controlling the battery. Below the five strategies are presented. All codes for HEM models and simulations are openly available at Ref. [47].

Self-consumption maximization (SCM). SCM was used as the benchmark method in this study. It is a rule-based algorithm with the objective of maximizing self-consumed production. This means that self-consumption of PV is prioritized, then charging of battery with excess PV production and discharging battery to load, and lastly grid exports/imports if battery is full/empty. The algorithm is described in literature with all the details in [19] (Algorithm 1), the only exceptions being our hourly resolution instead of 30-min resolution and initial battery charge of 0 kWh instead of half charged battery.

Model predictive control (MPC). We implemented MPC by solving the optimization on a given hour h with forecasted hours from h to $h+24$ using MILP. For solving the MILP, we used Gurobi solver (version 12.0.2) with gurobipy library (version 12.0.3) for Python. The 24-hour optimization horizon was used, because it is commonly used [18,20,24] and since it includes the whole day-and-night cycle. For the load and the PV production, we used Naïve forecasting by assuming the load to be the same as one week ago and production the same as one day ago. The day-ahead spot prices for next day are released each day at 13:45 Eastern European Time, leading to optimization horizon with a maximum of 14 unknown day-ahead spot prices (at 13:00). We filled these unknown times with Naïve forecasting, assuming the same prices as previous day on the same time.

On a given 24-hour period, we minimized the electricity bill over this period by minimizing the associated objective function:

$$\text{minimize} \sum_{t \in \mathcal{H}} C_{\text{el.bill}}(t) \tag{18}$$

$$C_{\text{el.bill}}(t) = p_{\text{purch}}(t) \cdot E_{\text{purch}}(t) - p_{\text{sell}}(t) \cdot E_{\text{sell}}(t), \tag{19}$$

where $\mathcal{H}$ is a set containing the 24 h that is optimized at a given moment, and E_{purch} and E_{sell} are the amounts of purchased and sold electric energy, respectively. As a result, the optimization gives the charge and discharge patterns over the 24-hour period. The optimization was performed under the constraints presented in the Supplementary Information Section S1.1. The algorithm is presented in the same section as well.

MPC with battery usage costs (MPC-BC). MPC with battery usage costs (MPC-BC) was applied by adding the battery usage costs to the cost function with electricity bill:

$$\text{minimize} \sum_{t \in \mathcal{H}} \left(C_{\text{el.bill}}(t) + C_{\text{BAT}}(t) \right). \tag{20}$$

Because linear MILP was used for optimization, the cyclic and float aging factor curves (Eqs. 10 and 14) were linearized. This linearization, optimization constraints, and the algorithm are presented in the Supplementary Information Section S1.2.

Reinforcement learning (RL). We applied a deterministic policy gradient method as the reinforcement model. The model is described in detail in Ref. [43]. Electricity bill was used as the loss function (Eq. (18)), which was minimized. The model output was charge and discharge pattern of the battery. Neural network (NN) with three hidden layers, each consisting of 100 neurons with rectified linear unit (ReLU) activation, was used as the policy function. The NN was implemented using the PyTorch library [74] (version 1.8.1). The input vector consisted of 78 variables, including PV production, load, electricity spot, purchase and sell prices, and the battery SOC on given time t, as well as day-ahead spot prices, forecasted load and production for next 24 h. The output was a scalar between [−1,1], negative values indicating battery discharge and positive values battery charging. To obtain the charge/discharge power, this output was scaled with the battery rated power of 5 kW. The model training was performed by minimizing the electricity bill over episodes with a length of one week, using Adam optimizer [75] with a learning rate of 10^{-4}. For training, data from March to September in 2020 were used. After the initial training, the NN was updated during the simulation every two weeks, using realized data from previous two weeks. This dynamic training allows the model to adapt to changing conditions.

RL with battery usage costs (RL-BC). We added the battery usage costs to the loss function of RL model, resulting in the same loss function than with MPC-BC (Eq. (20)). Model architecture, training, and implementation were otherwise similar to RL (see above).

3. Results and discussion

This section presents the simulation results for different loads and HEM strategies over the three years. First, the operation of each HEM strategy is demonstrated with a three-day example period in Section 3.1, after which the annual electricity bills and battery usage costs are shown for each scenario in Section 3.2. Section 3.3 presents the evaluation of break-even battery CAPEX to reach profitability, followed by the HEM strategies' effect on battery degradation and lifetime in Section 3.4. Lastly, we discuss on reaching the economic break-even point of battery in Section 3.5 and effects of battery degradation modeling in Section 3.6.

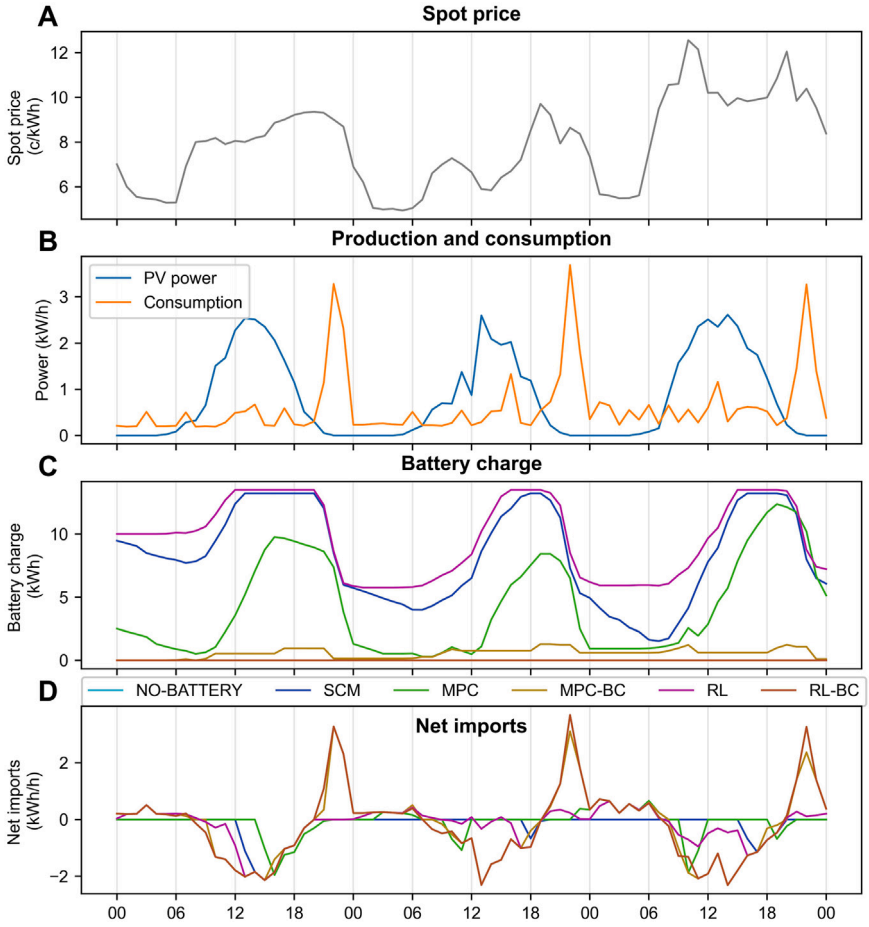

Fig. 6. Operational examples of the different energy management strategies with load L1 on 10–12th of July 2021. A: spot prices, B: PV production and consumption, C: battery charge of all strategies, D: net imports of all strategies. NO-BATTERY line overlaps with RL-BC and MPC-BC. NO-BATTERY: case with only PV and no battery, SCM: rule-based self-consumption maximization, MPC: optimization-based model predictive control, MPC-BC: MPC with battery usage costs in the loss function, RL: reinforcement learning, RL-BC: RL with battery usage costs in the loss function.

3.1. Operation (example days)

Fig. 6 shows the operation examples of the different HEM strategies with load L1 on a three-day-period from 10–12th of July in 2021. The same data is shown in Supplementary Information Figure S2 for each HEM strategy separately. These days were selected to represent mostly sunny summer days with distinct variation in spot prices. Based on the PV production (Fig. 6B), the first and third day were supposedly mostly sunny days, whereas some clouds were present in the second day. During the first two days, spot prices remained between 5 and 10 c/kWh, but during the third day, they elevated above 10 c/kWh (Fig. 6A). Regarding NO-BATTERY scenario, most of the production is sold to grid (negative net imports), since the consumption during day-time is low with load L1. The consumption peaks during the night, most probably due to the heating of the hot-water tank, when there is no PV production, leading to large amounts of purchased electricity from the grid.

When battery is added to the system, strategies with battery usage costs in their loss function (MPC-BC and RL-BC) leads to low to no battery cycling. This is because the battery usage costs from cycling the battery would be most of the time higher than the corresponding savings in the electricity bill.

With SCM, MPC, and RL, the battery cycles are large. A great amount of excess production is stored to the battery and used during the evening or night when there is no production. During all days, exports take place, which is due to limited storage capacity in the case of SCM and RL. However, MPC results in exports even when the battery is not full if those export times would minimize the electricity bill. A notable difference between the rule-based SCM and electricity bill minimizing MPC and RL is that with SCM, the battery charge is used during night-time to cover the consumption, leading to zero grid imports during the example period. However, MPC and RL utilize the diurnal variability in spot prices by buying electricity from the grid to cover consumption during night-time in order to preserve battery charge for day-times when spot prices are higher. Additionally, MPC and RL utilized the peak spot price hour during the morning of the third day by selling a little portion of the production instead of storing it all to the battery. However, their battery charging patterns differ since they are two different models which utilize two different approaches to minimize the same objective function.

3.2. Total costs

To evaluate the economic profitability of the different strategies, we calculated the total costs for each year and HEM strategy, shown in Fig. 7. When the annual battery usage costs due to degradation (described in Section 2.4) are added together with the annual electricity bill, the total costs of all HEM strategies and loads increased by 7%–60%, compared with corresponding NO-BATTERY reference scenarios. This increase in the total costs indicates that the battery is economically unfeasible addition to the system with the given battery CAPEX of 9000 EUR (667 EUR/kWh). Considering the strategies with batteries, RL-BC and MPC-BC reached the lowest total costs. Their loss function manifests a tradeoff between grid import and battery usage costs, joint

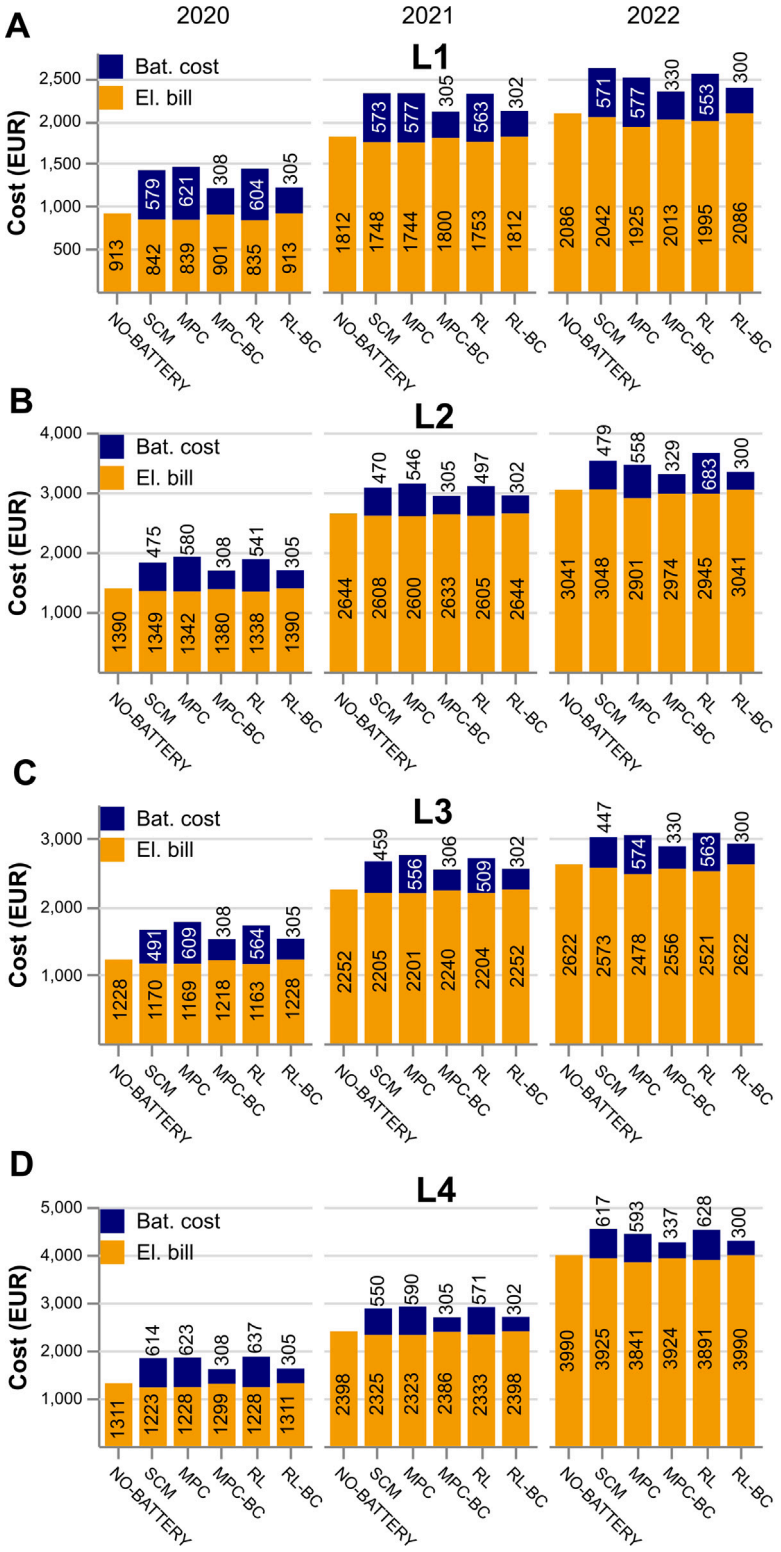

Fig. 7. Electricity bills (El. bill) and battery usage costs due to battery degradation (Bat. cost) of A: load L1, B: load L2, C: load L3, and D: load L4. NO-BATTERY: case with only PV and no battery, SCM: rule-based self-consumption maximization, MPC: optimization-based model predictive control, MPC-BC: MPC with battery usage costs in the loss function, RL: reinforcement learning, and RL-BC: RL with battery usage costs in the loss function.

optimization of which results in minimized total expenses. However, because of the high battery CAPEX, this resulted in a strategy that the battery is hardly used at all, as was shown in Fig. 6. Especially with RL-BC, the battery throughput was zero over the simulation period in all cases, in which case the electricity bill was equal to NO-BATTERY and the battery usage costs were due to the float aging only. With MPC-BC, the battery was used if the savings in the electricity bill of a given 24-hour optimization horizon with forecast inputs were greater than the corresponding battery usage costs. This strategy led to low savings and low battery usage. Since these two independent approaches of MPC-RL

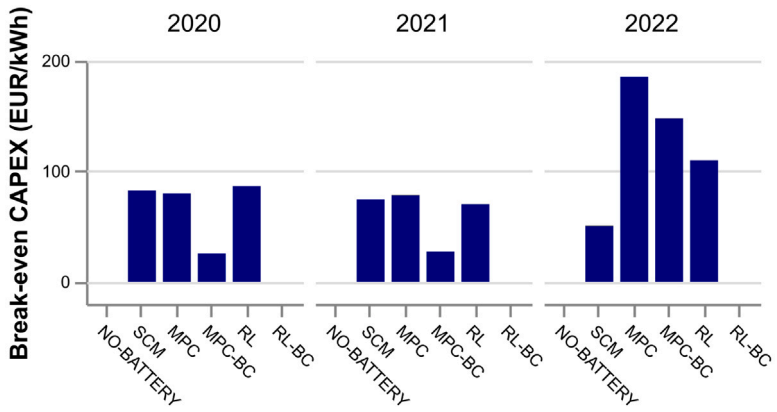

Fig. 8. Break-even capital expenses (CAPEX) with load L1 for the given 13.5 kWh battery. RL-BC values are zero because no savings in electricity bill were made with that strategy. SCM: rule-based self-consumption maximization, MPC: optimization-based model predictive control, MPC-BC: MPC with battery usage costs in the loss function, RL: reinforcement learning, and RL-BC: RL with battery usage costs in the loss function.

and RL-BC both lead to similar strategy and results, we can conclude that these total costs are near the annual minimum.

Annual savings in electricity bills were in most cases in the range of tens of euros with added battery, and there were only minor differences between SCM, MPC, and RL during 2020 and 2021, when the spot prices were low. Table S4, shown in the Supplementary Information, presents the relative differences of electricity bills of MPC and RL compared with SCM. The reduction in electricity bills with MPC and RL is only 0.8% at highest compared with the simple SMC during 2020 and 2021. When spot prices and diurnal variability in the prices increased through 2021 to 2022 (see Fig. 4), RL, and especially MPC, resulted in increased savings compared with SCM, around 5.7% at highest. Over the three-year period, MPC led to only around 2% lower electricity bills, and RL resulted in savings under 1%, compared with SCM. This quite small difference is probably due to the generally low electricity prices in Finland and also due to limited possibilities to create additional savings with battery: here, battery charging is limited only to PV production, which reaches its peak during daytime, when the electricity prices also peak. In literature, over 10% cost reductions are reported with more advanced methods over SCM [20,21], but those consider the total costs, including the electricity bill and battery usage costs. In fact, in [20], the electricity bill was lower with SCM compared with the economic optimization method, but the battery usage costs were significantly higher. Considering the total costs here in our work, MPC-BC and RL-BC reduce the total costs also somewhere around 10% compared with SCM.

The greatest savings in electricity bill occurred during 2022, where maximum annual savings in electricity bill of 161 EUR were obtained with load L1 (Fig. 7A) and MPC. However, the corresponding battery usage costs were 577 EUR. To estimate the lowest possible electricity bills, we applied MILP with the same constraints used in MPC, to optimize the whole years using the realized historical values and neglecting battery degradation. With this yearly optimization, the annual electricity bills were 58–260 EUR lower compared with the lowest electricity bills presented in Fig. 7, the lowest difference occurring in 2020 and the highest difference in 2022. The data is shown in Supplementary Information Section S4. However, even if the electricity bills would be 260 EUR lower than those shown in Fig. 7, the battery usage costs would still remain too high for the battery to be profitable. To reach economic break-even point, the annual savings in electricity bill should be at least over 500 EUR, which is the magnitude of battery usage costs when battery is utilized (SCM, MPC, RL, and yearly MILP in Figure S3).

These savings in electricity bills are generally rather low, caused especially by the low electricity prices in Finland and the diurnal match of electricity prices and PV production. The added battery saves mostly the night-time consumption, when the electricity prices reach their lowest values (see Fig. 4). With L2 (Fig. 7B), SCM actually caused even higher electricity bill than with NO-BATTERY during 2022 (3048 EUR and 3041 EUR, respectively). This means that in this case, adding a battery increased the electricity bill, which is very unexpected. The elevated electricity bill was caused by storing the excess production to battery during daytime, therefore preventing high revenues from selling this production. Using the battery charge during night-time resulted in only low savings, since the electricity price was significantly lower during nights. This result highlights the importance of including the spot price information in the decision making if there is large variability in electricity prices. With other loads, SCM always lowered the electricity bills compared with NO-BATTERY.

3.3. Battery break-even CAPEX

Fig. 8 presents the break-even battery CAPEXes evaluated for load L1 for each year and strategy, using Eq. (17). Results for other loads were similar, and they are presented in Supplementary Information Section S5. Break-even values for NO-BATTERY were zero, because this strategy did not have a battery. RL-BC resulted in break-even values of zero, since it did not produce any electricity bill savings. Similarly, MPC-BC lead to low break-even values due to low battery throughput. However, during 2022, the break-even values obtained with MPC-BC are distinctly higher, since there were more occasions, where using the battery lead to higher savings than the corresponding battery usage costs. It should be noted that these break-even values for MPC-BC and RL-BC are not really representative, since the battery CAPEX affects the battery operation, and therefore changing the CAPEX would affect the battery throughput and electricity bill savings.

SCM, MPC, and RL resulted in similar break-even values between 50 to 100 EUR/kWh during years 2020 and 2021, depending on the load. These break-even CAPEXes are correspondingly over 6 to 13 times smaller than the used CAPEX of 667 EUR/kWh. During 2022, MPC and RL had elevated break-even CAPEXes due to larger electricity bill savings. Especially, MPC resulted in the highest break-even CAPEX of 185 EUR/kWh (this is highest among all loads, see Section S5), despite the heaviest battery usage (highest battery usage costs in Fig. 7). This result suggests that the value of battery is maximized by its high utilization. When battery is in the idle-state, it is still affected by the float aging while not producing any savings. Therefore, all times when the battery is not producing any savings, are wasting battery life. During the winters, the battery is practically always in the idle-mode because of the low PV production, and this lowers the profitability of the battery.

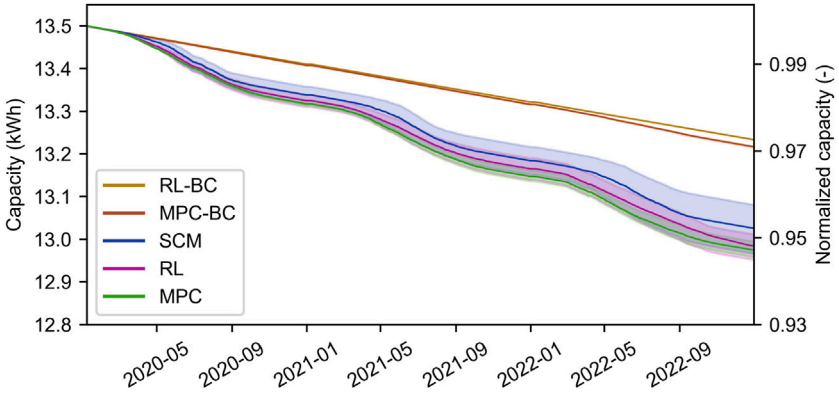

Fig. 9. The battery capacity as a function of time over the simulation period. Each strategy is presented with different color, where the width of the color represents the interval containing all batteries for each load, and the line in the middle of the color represents the mean of the interval. SCM: rule-based self-consumption maximization, MPC: optimization-based model predictive control, MPC-BC: MPC with battery usage costs in the loss function, RL: reinforcement learning, and RL-BC: RL with battery usage costs in the loss function.

3.4. Battery degradation and lifetime

To understand how the different HEM strategies affect the battery degradation, we assessed the capacity time-series of the batteries for each strategy, depicted in Fig. 9. The capacities with MPC-BC and RL-BC decreased linearly, because the batteries stayed unused (or nearly unused, in the case with MPC-BC) and thus they were subjected only to similar linear float degradation. Other strategies resulted in a wavy degradation pattern, where summers led to faster capacity losses and winter times slower losses. This pattern occurs because cyclic aging leads to faster degradation than float aging, on average, and during winter times the batteries were not cycled. MPC lead to the fastest degradation, as was already seen from the highest battery usage costs of MPC in Fig. 7. At highest, the capacity decreased over 5% after the three-year period. Heavier battery usage of MPC over SCM is because MPC can charge the battery even in cases where all production could be self-consumed, unlike SCM. RL on the other hand lead to higher float aging compared to other strategies. As we showed in Fig. 6C, the battery remained partly charged long periods of times, causing higher float degradation. The annual ΔSOH divided to cyclic and float aging for each strategy and load are presented in the Supplementary Information Section S6.

Based on the degradation of the three-year period, we estimated the projected battery lifetimes, presented in Fig. 10. Lifetime means the operational time after which a battery has reached its EoL, *i.e.*, a capacity fade of 20% from the original capacity of 13.5 kWh. In nearly all scenarios, the projected lifetime is above 15 years. With MPC-BC and RL-BC, the lifetimes are around 30 years, since the batteries stay nearly or completely unused. MPC and RL lead to the shortest lifetimes, because of their heaviest battery utilization.

3.5. Discussion on reaching the economic break-even point

The highest break-even CAPEX was 185 EUR/kWh, obtained with MPC and load L1 under high and volatile prices during 2022. This value is over 3.5 times smaller than the used CAPEX of 667 EUR/kWh, implying that the CAPEX should be significantly lower with the given electricity prices and degradation model for the battery to be economically viable. There are cheaper alternatives in the markets compared with the battery used in this work, such as the 15 kWh Li-iron phosphate battery-pack by DianKaiShou with a price of 1491 EUR (100 EUR/kWh) [76]. However, adding costs for inverter, installation, and management system would raise the total CAPEX most likely over the highest break-even value of 185 EUR/kWh. Additionally, National Renewable Energy Laboratory (NREL) has estimated battery CAPEX as low as 2580 USD for 12.5 kWh/5 kW battery in US [77], leading to

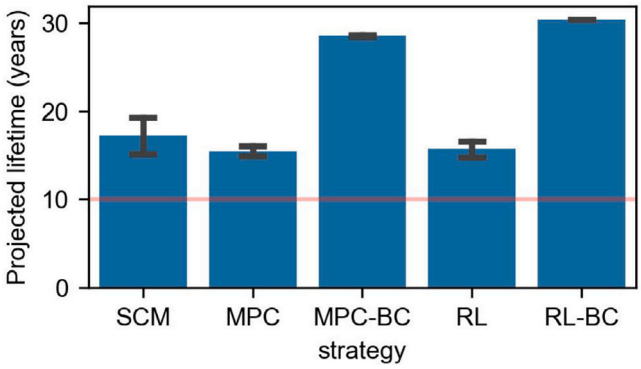

Fig. 10. Projected lifetimes until 20% capacity loss for each strategy. The height of a bar represents the mean lifetime over all loads, and errorbars on each bar represent the minimum and maximum value. The red line at 10 years indicate the warranty by manufacturer. SCM: rule-based self-consumption maximization, MPC: optimization-based model predictive control, MPC-BC: MPC with battery usage costs in the loss function, RL: reinforcement learning, and RL-BC: RL with battery usage costs in the loss function.

CAPEX of 206 USD/kWh ≈ 190 EUR/kWh (with a rate of 1 USD=0.91 EUR). This implies that even cheaper alternatives are too expensive to be economically profitable in the case of this study, even under high electricity prices during the energy crisis.

The results in this work showed that adding a battery to existing residential systems with PV is economically unprofitable when storing the produced PV electricity is the sole purpose of the battery. In addition to battery CAPEX, one major reason is the low electricity prices of Finland. For example, Berglund et al. [45] demonstrated that adding a battery to a swimminghall with an existing PV system in Norway is economically viable. However, they had a fixed feed-in tariff of 0.04 NOK/kWh (≈ 0.4 c/kWh in the publication year 2018 [78]), which is over 10 times lower than the total cost of purchased energy of 0.41 NOK/kWh (≈ 4.1 c/kWh [78]) (928,719 NOK/2,243,653 kWh), where the total costs included cost of purchased energy and peak power tariffs. This large difference in the prices favors self-consumption, and with a battery, the peak feed-in power could be lowered, thus reducing the peak power tariffs. However, in our Finnish case, the annual mean electricity purchase price was at its highest only around 3.7 times greater than the mean feed-in price during 2020, when the mean purchase price was 9.19 c/kWh and selling price was 2.49 c/kWh (see Table 1). Together with low spot prices in general, the savings in the electricity bill with the battery remained low. To summarize, at best,

the saving in electricity bill were low compared to the battery usage cost. At worst, the added battery could even lead to higher electricity bills than a system without a battery, as was shown in Fig. 7B, under the extreme case in 2022.

The increasing number of days with negative electricity prices can increase the profitability of residential battery with PV in the future, since energy storage can help to prevent economic losses from selling excess production under these negative prices. However, based on the low savings and a very large gap to reach profitability presented in this work, it is likely that adding a battery remains economically unprofitable, regardless of the negative spot prices. However, there are other reasons outside economic profitability, why one would install a battery to their home, such as self-sufficiency and energy resilience, which we have omitted in this work.

We concluded that the low break-even battery CAPEXes are partly affected by the low battery utilization during winters. These break-even values could be increased by allowing battery charging directly from grid, thus creating savings throughout the year and minimizing the battery idle-time. However, based on our previous work [79], the increased battery usage costs resulting from this type of grid connection are much greater than the electricity bill savings, and thus it is economically unfeasible. Additionally, taking part in electricity reserve markets with home batteries is becoming more popular, and could allow additional profits [80].

3.6. Discussion on the battery lifetime and effect of degradation modeling

The obtained lifetimes of 15–20 years are in the typical range, considering other literature works. From example, Azuatalam et al. [19] reported battery lifetimes mostly between 10 and 20 years for over 50 residential customers with variable sizes PV (3–10 kWp) and batteries (6.5–14 kWh) with various energy management strategies in Australia. Magnor et al. [68] showed battery lifetimes between 9 and 22 years by varying the size of the battery from 1 to 10 kWh, when they applied their degradation model (the same model we used in this work) to a residential case with a 5 kWp PV system, 4 MWh annual consumption, and SCM energy management in Germany. Battery lifetimes could be extended by lowering the EoL. For example, assuming an EoL at 60% of initial capacity instead of the used 80% would lead to doubled battery lifetime. For stationary battery applications, such as home batteries, lower EoL could be used, since the specific energy (kWh/kg) requirements are less strict compared with electric vehicle batteries.

The battery degradation model has a great impact on the lifetimes. If we had used a degradation model with halved degradation rates, or assumed an EoL of 60%, the break-even CAPEXes would have doubled, leading to a maximum CAPEX of 370 EUR/kWh. This CAPEX is over the estimated cheapest battery system CAPEX in US [77]. However, this doubling of CAPEXes would lead to break-even CAPEX around 100–200 EUR/kWh under more typical electricity prices in 2020 and 2021, making the added battery still likely unprofitable. Thus, for the addition of the battery to become economically feasible, the costs of the battery systems should be lowered (possibly through the usage of second-life batteries), the lifetimes should be longer (*e.g.*, by lowering the EoL), and electricity price should be similar than during energy crisis in 2022.

4. Conclusions

This work presented a comprehensive study on adding a battery to residential households with existing PV in a Finnish residential context. The novel contribution was the inclusion of battery usage costs and degradation in the energy management under dynamic spot prices over a period of three years with a drastically varying electricity price. More precisely, we analyzed five different HEM strategies, two of which considered battery degradation in the decision making, using real PV production and four real residential electricity consumption profiles. Electricity bills were based on dynamic spot pricing under three electricity price years, spanning from COVID-time (2020 and 2021) to energy crisis (2022) prices. Our objectives were to discover if (1) adding a battery is economically feasible and (2) how much different HEM strategies for battery scheduling affect the total costs.

For our first objective, we showed that adding a 13.5 kWh/9000 EUR battery to the studied systems was economically unfeasible. We obtained the highest economic break-even battery CAPEX of 185 EUR/kWh during year 2022 with high spot prices, but it is over 3.5 times lower than the given CAPEX of 667 EUR/kWh. Compared with NO-BATTERY, the highest electricity bill savings were 161 EUR/year (obtained during 2022), with corresponding battery usage costs of 577 EUR/year.

Regarding our second objective, years 2020 and 2021 showed only small differences in electricity bills between simple rule-based SCM and more complex MPC and RL strategies. MPC and RL lowered the electricity bill only 0.8% at highest, compared with SCM. These savings over SCM were surprisingly low, since MPC and RL were based on minimizing the electricity bill. During 2022 under elevated spot prices and huge diurnal variability in the price, MPC and RL showed lower electricity bills compared with SCM, 5.7% at highest. In one case in 2022, the added battery with SCM strategy actually increased the electricity bill from NO-BATTERY case, which is very unexpected result. When battery usage costs were applied to the cost function of MPC-BC and RL-BC, batteries remained practically unused due to high battery usage costs. Since these two independent approaches lead to this trivial strategy, we concluded that the total costs obtained with those strategies are near the annual minimum.

To reach economic profitability of home batteries, the break-even CAPEX should increase significantly, when considering current electricity prices. The gap between the break-even and current battery CAPEX is large and thus single large improvements are insufficient to approach the economic break-even. Instead, several major changes are likely needed: for instance, using significantly lower EoL, and simultaneously reaching high electricity prices similar to 2022, would lead to break-even CAPEX near the CAPEXes of available battery systems in the markets. Analysis of second life batteries and their potential to reach lower CAPEX could be interesting future study. Increased spot prices and greater differences between purchase and selling prices would increase this break-even value. However, batteries can improve the resilience of a household during power shortages and provide value beyond the economic savings by, *e.g.*, allowing electrification off the grid, if they are configured appropriately. The present study enables evaluating if these other values are worth the added costs of a battery system.

CRediT authorship contribution statement

Lauri Karttunen: Writing – review & editing, Writing – original draft, Software, Methodology, Formal analysis, Data curation, Conceptualization. **Sami Jouttijärvi:** Writing – review & editing, Supervision, Methodology, Conceptualization. **Jerzy J. Jasielec:** Writing – review & editing, Writing – original draft, Methodology. **Johannes Niskanen:** Writing – review & editing, Methodology. **Hugo Huerta:** Resources, Data curation. **Samuli Ranta:** Writing – review & editing, Resources. **Kati Miettunen:** Writing – review & editing, Supervision, Funding acquisition, Conceptualization.

Declaration of Generative AI and AI-assisted technologies in the writing process

During the preparation of this work the author(s) used MS Copilot in order to condense the abstract to fit the given word limit. After using this tool/service, the author(s) reviewed and edited the content as needed and take(s) full responsibility for the content of the publication.

Declaration of competing interest

The authors declare that they have no known competing financial interests or personal relationships that could have appeared to influence the work reported in this paper.

Acknowledgments

The work was funded by the University of Turku and the city of Salo (LK, JJ), Finland, and Strategic Research Council within the Research Council of Finland, Decision No. 358542 (KM, SJ, LK) and Decision No. 359141 (SR, HH). LK is also grateful for the funding from the University of Turku Graduate School (UTUGS), Finland.

Appendix A. Supplementary data

Supplementary material related to this article can be found online at https://doi.org/10.1016/j.est.2026.121301.

Data availability

PV production data used in this work can be found at [49]. All codes for HEM models and simulations are available at [47]. The authors do not have permission to share consumption data.

References

[1] Fingrid, Solar power, 2025, (Accessed 12 March 2025). URL https://www.fingrid.fi/en/electricity-market-information/solar-power.

[2] Renewables Finland, Suunnittelussa olevat aurinkovoimalahankkeet, 2025, (Accessed 31 March 2025). URL https://suomenuusiutuvat.fi/aurinkovoima/aurinkovoimahankkeet-ja-voimalat-suomessa/suunnittelussa-olevat-aurinkovoimahankkeet/.

[3] S. Jouttijärvi, L. Karttunen, S. Ranta, K. Miettunen, Techno-economic analysis on optimizing the value of photovoltaic electricity in a high-latitude location, Appl. Energy 361 (2024) 122924, http://dx.doi.org/10.1016/J.APENERGY.2024.122924.

[4] X. Han, J. Garrison, G. Hug, Techno-economic analysis of PV-battery systems in Switzerland, Renew. Sustain. Energy Rev. 158 (2022) 112028, http://dx.doi.org/10.1016/j.rser.2021.112028.

[5] S. Schopfer, V. Tiefenbeck, T. Staake, Economic assessment of photovoltaic battery systems based on household load profiles, Appl. Energy 223 (2018) 229–248, http://dx.doi.org/10.1016/j.apenergy.2018.03.185.

[6] J. Linssen, P. Stenzel, J. Fleer, Techno-economic analysis of photovoltaic battery systems and the influence of different consumer load profiles, Appl. Energy 185 (2017) 2019–2025, http://dx.doi.org/10.1016/j.apenergy.2015.11.088.

[7] P. Puranen, A. Kosonen, J. Ahola, Techno-economic viability of energy storage concepts combined with a residential solar photovoltaic system: A case study from Finland, Appl. Energy 298 (2021) 117199, http://dx.doi.org/10.1016/j.apenergy.2021.117199.

[8] A. Chaianong, A. Bangviwat, C. Menke, B. Breitschopf, W. Eichhammer, Customer economics of residential PV–battery systems in Thailand, Renew. Energy 146 (2020) 297–308, http://dx.doi.org/10.1016/J.RENENE.2019.06.159.

[9] L. Pereira, J. Cavaleiro, L. Barros, Economic Assessment of Solar-Powered Residential Battery Energy Storage Systems: The Case of Madeira Island, Portugal, Appl. Sci. 2020, Vol. 10, Page 7366 10 (20) (2020) 7366, http://dx.doi.org/10.3390/APP10207366.

[10] O. Alavi, J. Despeghel, W.D. Ceuninck, M. Meuris, J. Driesen, M. Daenen, Economic Study of Battery Profitability in Residential Solar Panel Systems: A Case Study of Belgium, Proc. - 2020 IEEE 14th Int. Conf. Compat. Power Electron. Power Eng. CPE-POWERENG 2020 (2020) 358–363, http://dx.doi.org/10.1109/CPE-POWERENG48600.2020.9161506.

[11] H.S. Nygård, S.Ø. Ottesen, O.H. Skonnord, Profitability Analyses for Residential Battery Investments: A Norwegian Case Study, Energies 2024, Vol. 17, Page 4048 17 (16) (2024) 4048, http://dx.doi.org/10.3390/EN17164048.

[12] B. Zakeri, S. Cross, P. Dodds, G.C. Gissey, Policy options for enhancing economic profitability of residential solar photovoltaic with battery energy storage, Appl. Energy 290 (2021) 116697, http://dx.doi.org/10.1016/j.apenergy.2021.116697.

[13] B. Lin, W. Wu, Economic viability of battery energy storage and grid strategy: A special case of China electricity market, Energy 124 (2017) 423–434, http://dx.doi.org/10.1016/j.energy.2017.02.086.

[14] Y.S. Son, T. Pulkkinen, K.D. Moon, C. Kim, Home energy management system based on power line communication, IEEE Trans. Consum. Electron. 56 (3) (2010) 1380–1386, http://dx.doi.org/10.1109/TCE.2010.5606273.

[15] B. Zhou, W. Li, K.W. Chan, Y. Cao, Y. Kuang, X. Liu, X. Wang, Smart home energy management systems: Concept, configurations, and scheduling strategies, Renew. Sustain. Energy Rev. 61 (2016) 30–40, http://dx.doi.org/10.1016/J.RSER.2016.03.047.

[16] A.O. Ali, M.R. Elmarghany, M.M. Abdelsalam, M.N. Sabry, A.M. Hamed, Closed-loop home energy management system with renewable energy sources in a smart grid: A comprehensive review, J. Energy Storage 50 (2022) 104609, http://dx.doi.org/10.1016/j.est.2022.104609.

[17] B. Han, Y. Zahraoui, M. Mubin, S. Mekhilef, M. Seyedmahmoudian, A. Stojcevski, Home Energy Management Systems: A Review of the Concept, Architecture, and Scheduling Strategies, IEEE Access 11 (2023) 19999–20025, http://dx.doi.org/10.1109/ACCESS.2023.3248502.

[18] M. Beaudin, H. Zareipour, Home energy management systems: A review of modelling and complexity, Renew. Sustain. Energy Rev. 45 (2015) 318–335, http://dx.doi.org/10.1016/J.RSER.2015.01.046.

[19] D. Azuatalam, K. Paridari, Y. Ma, M. Förstl, A.C. Chapman, G. Verbič, Energy management of small-scale PV-battery systems: A systematic review considering practical implementation, computational requirements, quality of input data and battery degradation, Renew. Sustain. Energy Rev. 112 (2019) 555–570, http://dx.doi.org/10.1016/J.RSER.2019.06.007, arXiv:1905.09498.

[20] B. Zou, J. Peng, R. Yin, Z. Luo, J. Song, T. Ma, S. Li, H. Yang, Energy management of the grid-connected residential photovoltaic-battery system using model predictive control coupled with dynamic programming, Energy Build. 279 (2023) 112712, http://dx.doi.org/10.1016/J.ENBUILD.2022.112712.

[21] G. Angenendt, S. Zurmühlen, H. Axelsen, D.U. Sauer, Comparison of different operation strategies for PV battery home storage systems including forecast-based operation strategies, Appl. Energy 229 (2018) 884–899, http://dx.doi.org/10.1016/J.APENERGY.2018.08.058.

[22] M.A. Hossain, H.R. Pota, S. Squartini, F. Zaman, J.M. Guerrero, Energy scheduling of community microgrid with battery cost using particle swarm optimisation, Appl. Energy 254 (2019) 113723, http://dx.doi.org/10.1016/J.APENERGY.2019.113723.

[23] Z. Luo, J. Peng, Y. Tan, R. Yin, B. Zou, M. Hu, J. Yan, A novel forecast-based operation strategy for residential PV-battery-flexible loads systems considering the flexibility of battery and loads, Energy Convers. Manage. 278 (2023) 116705, http://dx.doi.org/10.1016/j.enconman.2023.116705.

[24] T.H.B. Huy, H. Truong Dinh, D. Ngoc Vo, D. Kim, Real-time energy scheduling for home energy management systems with an energy storage system and electric vehicle based on a supervised-learning-based strategy, Energy Convers. Manage. 292 (2023) 117340, http://dx.doi.org/10.1016/j.enconman.2023.117340.

[25] I. Gomes, M. Ruano, A. Ruano, MILP-based model predictive control for home energy management systems: A real case study in algarve, Portugal, Energy Build. 281 (2023) 112774, http://dx.doi.org/10.1016/j.enbuild.2023.112774.

[26] J. Hu, Y. Shan, J.M. Guerrero, A. Ioinovici, K.W. Chan, J. Rodriguez, Model predictive control of microgrids – An overview, Renew. Sustain. Energy Rev. 136 (2021) 110422, http://dx.doi.org/10.1016/J.RSER.2020.110422.

[27] M. Beaudin, H. Zareipour, A. Schellenberg, Residential energy management using a moving window algorithm, IEEE PES Innov. Smart Grid Technol. Conf. Eur. (2012) http://dx.doi.org/10.1109/ISGTEUROPE.2012.6465896.

[28] J. Cao, D. Harrold, Z. Fan, T. Morstyn, D. Healey, K. Li, Deep Reinforcement Learning-Based Energy Storage Arbitrage with Accurate Lithium-Ion Battery Degradation Model, IEEE Trans. Smart Grid 11 (5) (2020) 4513–4521, http://dx.doi.org/10.1109/TSG.2020.2986333.

[29] L. Yao, P.-Y. Liu, J. Teo, Hierarchical multi-agent deep reinforcement learning with adjustable hierarchy for home energy management systems, Energy Build. 331 (2025) 115391, http://dx.doi.org/10.1016/j.enbuild.2025.115391.

[30] X. Xu, Y. Jia, Y. Xu, Z. Xu, S. Chai, C.S. Lai, A Multi-Agent Reinforcement Learning-Based Data-Driven Method for Home Energy Management, IEEE Trans. Smart Grid 11 (4) (2020) 3201–3211, http://dx.doi.org/10.1109/TSG.2020.2971427.

[31] E. Mocanu, D.C. Mocanu, P.H. Nguyen, A. Liotta, M.E. Webber, M. Gibescu, J. Slootweg, On-Line Building Energy Optimization Using Deep Reinforcement Learning, IEEE Trans. Smart Grid 10 (4) (2019) 3698–3708, http://dx.doi.org/10.1109/TSG.2018.2834219, arXiv:1707.05878.

[32] T. Yu, D.S. Kim, S.-Y. Son, Optimization of scheduling for home appliances in conjunction with renewable and energy storage resources, Int. J. Smart Home 7 (4) (2013) URL https://www.researchgate.net/publication/284801242.

[33] C.O. Adika, L. Wang, Smart charging and appliance scheduling approaches to demand side management, Int. J. Electr. Power Energy Syst. 57 (2014) 232–240, http://dx.doi.org/10.1016/J.IJEPES.2013.12.004.

[34] T. Dias de Lima, P. Faria, Z. Vale, Optimizing home energy management systems: A mixed integer linear programming model considering battery cycle degradation, Energy Build. 329 (2025) 115251, http://dx.doi.org/10.1016/j.enbuild.2024.115251.

[35] M. Tostado-Véliz, H.M. Hasanien, R.A. Turky, Y.O. Assolami, D. Vera, F. Jurado, Optimal home energy management including batteries and heterogenous uncertainties, J. Energy Storage 60 (2023) 106646, http://dx.doi.org/10.1016/j.est.2023.106646.
[36] S. Lee, D.H. Choi, Reinforcement Learning-Based Energy Management of Smart Home with Rooftop Solar Photovoltaic System, Energy Storage System, and Home Appliances, Sensors 2019, Vol. 19, Page 3937 19 (18) (2019) 3937, http://dx.doi.org/10.3390/S19183937.
[37] L. Yu, W. Xie, D. Xie, Y. Zou, D. Zhang, Z. Sun, L. Zhang, Y. Zhang, T. Jiang, Deep Reinforcement Learning for Smart Home Energy Management, IEEE Internet Things J. 7 (4) (2020) 2751–2762, http://dx.doi.org/10.1109/JIOT.2019.2957289, arXiv:1909.10165.
[38] H. Ekhteraei Toosi, A. Merabet, A. Swingler, Impact of battery degradation on energy cost and carbon footprint of smart homes, Electr. Power Syst. Res. 209 (2022) 107955, http://dx.doi.org/10.1016/J.EPSR.2022.107955.
[39] K. Abdulla, J. De Hoog, V. Muenzel, F. Suits, K. Steer, A. Wirth, S. Halgamuge, Optimal Operation of Energy Storage Systems Considering Forecasts and Battery Degradation, IEEE Trans. Smart Grid 9 (3) (2018) 2086–2096, http://dx.doi.org/10.1109/TSG.2016.2606490.
[40] M.C. Bozchalui, S.A. Hashmi, H. Hassen, C.A. Cañizares, K. Bhattacharya, Optimal operation of residential energy hubs in smart grids, IEEE Trans. Smart Grid 3 (4) (2012) 1755–1766, http://dx.doi.org/10.1109/TSG.2012.2212032.
[41] J. Salpakari, P. Lund, Optimal and rule-based control strategies for energy flexibility in buildings with PV, Appl. Energy 161 (2016) 425–436, http://dx.doi.org/10.1016/J.APENERGY.2015.10.036.
[42] K. Shivam, J.C. Tzou, S.C. Wu, A multi-objective predictive energy management strategy for residential grid-connected PV-battery hybrid systems based on machine learning technique, Energy Convers. Manage. 237 (2021) 114103, http://dx.doi.org/10.1016/J.ENCONMAN.2021.114103.
[43] L. Karttunen, S. Jouttijärvi, J. Niskanen, J.J. Jasielec, H. Huerta, S. Ranta, K. Miettunen, Techno-economic analysis of residential PV-battery energy system in nordics, in: 41st European Photovoltaic Solar Energy Conference and Exhibition, 2024, 020507–001–020507–007, http://dx.doi.org/10.4229/EUPVSEC2024/5DV.2.1.
[44] L. Maeyaert, L. Vandevelde, T. Döring, Battery Storage for Ancillary Services in Smart Distribution Grids, J. Energy Storage 30 (2020) 101524, http://dx.doi.org/10.1016/J.EST.2020.101524.
[45] F. Berglund, S. Zaferanlouei, M. Korpas, K. Uhlen, Optimal Operation of Battery Storage for a Subscribed Capacity-Based Power Tariff Prosumer—A Norwegian Case Study, Energies 2019, Vol. 12, Page 4450 12 (23) (2019) 4450, http://dx.doi.org/10.3390/EN12234450.
[46] I. Ranaweera, O.M. Midtgård, Optimization of operational cost for a grid-supporting PV system with battery storage, Renew. Energy 88 (2016) 262–272, http://dx.doi.org/10.1016/J.RENENE.2015.11.044.
[47] L. Karttunen, Battery scheduling strategies for residential PV battery systems, 2026, (Accessed 24 February 2026). URL https://github.com/energy-systems-team/battery-scheduling-strategies-for-residential-PV-battery-systems.
[48] K. Solar, KD-P250W–280W, 2025, (Accessed 01 April 2025). URL https://cdn.enfsolar.com/Product/pdf/Crystalline/5927f03465ede.pdf.
[49] New Energy Research Center Turku, NERC Data Portal, 2026, (Accessed 24 February 2026). URL https://nerc.turkuamk.fi/data-portal/.
[50] S. Jouttijärvi, S. Seppälä, L. Karttunen, S. Ranta, S. Syri, K. Miettunen, Impact of growing national solar power capacity on the profitability of residential solar energy production in northern conditions, Renew. Energy 260 (2026) 125169, http://dx.doi.org/10.1016/j.renene.2025.125169.
[51] I. 61724-3, Photovoltaic system performance - Part 3: Energy evaluation method, 2016.
[52] I. 61724-1, Photovoltaic system performance – Part 1: Monitoring, 2021.
[53] Energiavirasto, Sähkön hintatilastot, 2024, (Accessed 01 June 2024). URL https://energiavirasto.fi/sahkon-hintatilastot.
[54] Tesla, Powerwall, 2025, (Accessed 01 April 2025). URL https://www.tesla.com/sites/default/files/pdfs/powerwall/Powerwall_2_AC_Datasheet_EN_NA.pdf.
[55] T. Maailma, Ikea alkaa myydä aurinkokennoja ja kotiakkuja – Asennetun akun hinta yli 2,5-kertainen Teslaan verrattuna, 2024, (Accessed 11 August 2024). URL https://tekniikanmaailma.fi/ikea-alkaa-myyda-aurinkokennoja-ja-kotiakkuja-asennetun-akun-hinta-yli-25-kertainen-teslan-verrattuna.
[56] J. Xie, X. Wei, X. Bo, P. Zhang, P. Chen, W. Hao, M. Yuan, State of charge estimation of lithium-ion battery based on extended Kalman filter algorithm, Front. Energy Res. Volume 11 (2023) http://dx.doi.org/10.3389/fenrg.2023.1180881.
[57] H. Bašić, V. Bobanac, H. Pandžić, Determination of Lithium-Ion Battery Capacity for Practical Applications, Batteries 9 (9) (2023) http://dx.doi.org/10.3390/batteries9090459.
[58] H. Solmaz, T. Kocakulak, Determination of lithium ion battery characteristics for hybrid vehicle models, Int. J. Automot. Sci. Technol. 4 (4) (2020) 264–271, http://dx.doi.org/10.30939/ijastech..723043.
[59] M. Kassem, C. Delacourt, Postmortem analysis of calendar-aged graphite/LiFePO4 cells, J. Power Sources 235 (2013) 159–171, http://dx.doi.org/10.1016/j.jpowsour.2013.01.147.
[60] M. Klett, R. Eriksson, J. Groot, P. Svens, K.C. Högström, R.W. Lindström, H. Berg, T. Gustafson, G. Lindbergh, K. Edström, Non-uniform aging of cycled commercial LiFePO4//graphite cylindrical cells revealed by post-mortem analysis, J. Power Sources 257 (2014) 126–137, http://dx.doi.org/10.1016/j.jpowsour.2014.01.105.
[61] C.R. Birkl, M.R. Roberts, E. McTurk, P.G. Bruce, D.A. Howey, Degradation diagnostics for lithium ion cells, J. Power Sources 341 (2017) 373–386, http://dx.doi.org/10.1016/j.jpowsour.2016.12.011.
[62] M. Lewerenz, J. Münnix, J. Schmalstieg, S. Käbitz, M. Knips, D.U. Sauer, Systematic aging of commercial lifepo4| graphite cylindrical cells including a theory explaining rise of capacity during aging, J. Power Sources 345 (2017) 254–263, http://dx.doi.org/10.1016/j.jpowsour.2017.01.133.
[63] M. Lewerenz, A. Warnecke, D.U. Sauer, Post-mortem analysis on lifepo4| graphite cells describing the evolution & composition of covering layer on anode and their impact on cell performance, J. Power Sources 369 (2017) 122–132, http://dx.doi.org/10.1016/j.jpowsour.2017.10.003.
[64] C. Weisenberger, B. Meir, S. Röhler, D.K. Harrison, V. Knoblauch, A post-mortem study of commercial 18650 lithium-ion cells with lini0. 5co0. 2mn0. 3o2//graphite chemistry after prolonged cycling (> 7000 cycles) with low C-rates, Electrochim. Acta 379 (2021) 138145, http://dx.doi.org/10.1016/j.electacta.2021.138145.
[65] P. Kuntz, O. Raccurt, P. Azaïs, K. Richter, T. Waldmann, M. Wohlfahrt-Mehrens, M. Bardet, A. Buzlukov, S. Genies, Identification of degradation mechanisms by post-mortem analysis for high power and high energy commercial li-ion cells after electric vehicle aging, Batteries 7 (3) (2021) 48, http://dx.doi.org/10.3390/batteries7030048.
[66] U. Mattinen, M. Klett, G. Lindbergh, R.W. Lindström, Gas evolution in commercial li-ion battery cells measured by on-line mass spectrometry–effects of C-rate and cell voltage, J. Power Sources 477 (2020) 228968, http://dx.doi.org/10.1016/j.jpowsour.2020.228968.
[67] L. Ellis, J. Allen, L. Thompson, J. Harlow, W. Stone, I. Hill, J. Dahn, Quantifying, understanding and evaluating the effects of gas consumption in lithium-ion cells, J. Electrochem. Soc. 164 (14) (2017) A3518, http://dx.doi.org/10.1149/2.0191714jes.
[68] D. Magnor, J.B. Gerschler, M. Ecker, P. Merk, D.U. Sauer, Concept of a battery aging model for lithium-ion batteries considering the lifetime dependency on the operation strategy, in: Proceedings of the European Photovoltaic Solar Energy Conference, Hamburg, Germany, 2009, pp. 21–25.
[69] H. Seiger, Effect of depth of discharge on cycle life of near-term batteries, in: 16th Intersociety Energy Conversion Engineering Conference, 1, 1981, pp. 102–110.
[70] A. Burke, Cycle Life Considerations for Batteries in Electric and Hybrid Vehicles, Tech. rep., SAE Technical Paper, 1995.
[71] L.H. Thaller, Expected cycle life vs. depth of discharge relationships of well-behaved single cells and cell strings, J. Electrochem. Soc. 130 (5) (1983) 986, http://dx.doi.org/10.1149/1.2119928.
[72] A. Bocca, A. Sassone, D. Shin, A. Macii, E. Macii, M. Poncino, An equation-based battery cycle life model for various battery chemistries, in: 2015 IFIP/IEEE International Conference on Very Large Scale Integration (VLSI-SoC), IEEE, 2015, pp. 57–62.
[73] M.A. Ortega-Vazquez, Optimal scheduling of electric vehicle charging and vehicle-to-grid services at household level including battery degradation and price uncertainty, IET Gener. Transm. Distrib. 8 (6) (2014) 1007–1016, http://dx.doi.org/10.1049/IET-GTD.2013.0624.
[74] A. Paszke, S. Gross, F. Massa, A. Lerer, J. Bradbury, G. Chanan, T. Killeen, Z. Lin, N. Gimelshein, L. Antiga, A. Desmaison, A. Kopf, E. Yang, Z. DeVito, M. Raison, A. Tejani, S. Chilamkurthy, B. Steiner, L. Fang, J. Bai, S. Chintala, PyTorch: An Imperative Style, High-Performance Deep Learning Library, in: H. Wallach, H. Larochelle, A. Beygelzimer, F. d'Alché Buc, E. Fox, R. Garnett (Eds.), Advances in Neural Information Processing Systems 32, Curran Associates, Inc., 2019, pp. 8024–8035, URL https://dl.acm.org/doi/10.5555/3454287.3455008.
[75] D.P. Kingma, J. Ba, Adam: A Method for Stochastic Optimization, 2017, http://dx.doi.org/10.48550/arXiv.1412.6980, ArXiv:1412.6980v9 [Cs.LG] arXiv:arXiv:1412.6980.
[76] AliExpress, DianKaiShou LiFePO4 CELL No.8, 2025, (Accessed 25 March 2025). URL https://www.aliexpress.com/item/1005008477007254.html?pdp_npi=4%40dis%21EUR%212.983%2C58%211.491%2C79%21%21%2122067.92%2111033.96%21%40211b6c891739356337212128e8826%21112000045318993490%21sh01%21FI%210%21X&spm=a2g0o.store_pc_home.productList_201161583.
[77] National Renewable Energy Laboratory (NREL), Annual Technology Baseline: Residential Battery Storage, 2025, (Accessed 06 April 2025). URL https://atb.nrel.gov/electricity/2024/residential_battery_storage.

[78] EXCHANGE-RATES.ORG, Norwegian Krone (NOK) To Euro (EUR) Exchange Rate History for 2018, 2025, (Accessed 01 April 2025). URL https://www.exchange-rates.org/exchange-rate-history/nok-eur-2018.

[79] L. Karttunen, Aurinkovoimalalla ja akulla varustetun kotitalouden energianhallinnan neuroverkkopohjainen optimointi, 2024, URL https://urn.fi/URN:NBN:fi-fe202402218213.

[80] G. Angenendt, M. Merten, S. Zurmühlen, D.U. Sauer, Evaluation of the effects of frequency restoration reserves market participation with photovoltaic battery energy storage systems and power-to-heat coupling, Appl. Energy 260 (2020) 114186, http://dx.doi.org/10.1016/j.apenergy.2019.114186.